

# Complexation between a Hydrophobically Modified Chitosan and Cyclodextrin Homodimers Singly or Doubly Connected through Their Primary Sides: Effects of Their Molecular Architecture on the Polymer Properties in Solution

Thomas Lecourt,<sup>†</sup> Pierre Sinaÿ,<sup>†</sup> Christophe Chassenieux,<sup>‡</sup>  
Marguerite Rinaudo,<sup>§</sup> and Rachel Auzély-Velty\*,<sup>§</sup>

*Ecole Normale Supérieure, Département de Chimie, UMR CNRS 8642 24, rue Lhomond, 75231 Paris, Cedex 05, France; Physicochimie des Polymères et des Milieux Dispersés, UMR CNRS 7615, ESPCI 10, rue Vauquelin 75231 Paris, Cedex 05, France; and Centre de Recherches sur les Macromolécules Végétales (CNRS), Université Joseph Fourier de Grenoble, BP 53, 38041 Grenoble Cedex, France*

Received January 27, 2004; Revised Manuscript Received April 7, 2004

**ABSTRACT:** The complexation properties toward adamantane-grafted chitosan of two  $\beta$ -cyclodextrin (CD) homodimers, containing two CD moieties that are linked through their primary sides by one or two aliphatic spacers, are studied by rheological and dynamic light scattering measurements. Very different behaviors are observed between these two CD molecules which can be related to different molecular flexibilities and inclusion properties of their cavities. These results show that a subtle change in the molecular architecture of such CD dimers dramatically changes their ability to physically cross-link modified chitosan chains.

## Introduction

Cyclodextrins are water-soluble cyclic oligosaccharides consisting of six ( $\alpha$ -CD), seven ( $\beta$ -CD), eight ( $\gamma$ -CD), or more D-glucopyranose units. In aqueous solution, their relatively hydrophobic cavity can accommodate a wide range of small organic molecules as guests leading to modification of their physicochemical properties, particularly in terms of water solubility and chemical stability.<sup>1,2</sup> For this reason, cyclodextrins have been extensively investigated for their use as carriers in various industries. These host molecules are also very interesting candidates for the development of catalytic systems,<sup>3</sup> sensor devices,<sup>4</sup> or molecular materials based on nano-organized systems.<sup>5</sup> Recently, we thus prepared original supramolecular assemblies in aqueous solution based on specific interactions between  $\beta$ -CD grafted on chitosan and adamantane attached to chitosan or poly(ethylene glycol).<sup>5e</sup> We demonstrated that the CD–adamantane complexes play the role of interchain junctions, leading to a large increase of the viscosity or the formation of temporary networks, depending on the guest macromolecule. In the present paper, we investigate the interaction between adamantane grafted chitosan **1** (Figure 1) and two  $\beta$ -cyclodextrin dimers **2a** and **2b**, containing two CD moieties connected on the primary side by one or two C8 aliphatic chains (Figure 2). There is currently great interest in such CD derivatives because favorable cooperative binding effects, due to multivalency, may occur, leading to significantly higher binding constants compared to the monomeric species.<sup>6</sup> Nevertheless, although a wide variety of analytical techniques can be used to investigate CD inclusion processes, the respective roles of solution conformations, steric effects, stabilizing interactions,

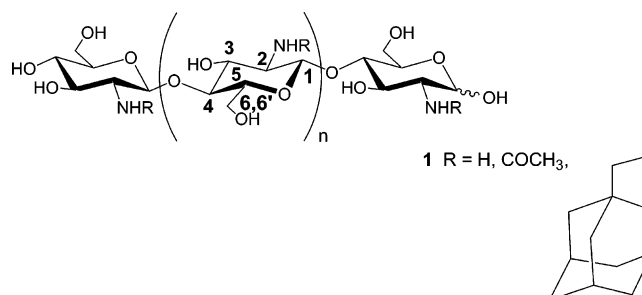


**Figure 1.** Structure of adamantane-grafted chitosan **1**.

and molecular rigidity on the complexation properties may not be easily evidenced for complex CD derivatives such as these CD dimers. In this study, rheology was shown to be a very sensitive technique to demonstrate the large influence of the nature of the linkage between the two CD cavities on the complexation properties of the CD derivatives. In the first section of this paper, the inclusion properties of these CD dimers and natural  $\beta$ -CD toward small organic molecules are compared. In the second section, we report on the complexation behavior of these CD derivatives toward adamantane-grafted chitosan as a guest macromolecule.

## Experimental Section

**Materials.** Adamantane-grafted chitosan with a degree of substitution equal to 0.05 was synthesized as previously reported.<sup>5e</sup> The parent chitosan used has a weight-average molecular weight  $M_w$  of 195 000; it is a commercial sample from Pronova (Norway) with a degree of N-acetylation equal to 0.12. The overlap concentration  $C^*$  for this chitosan sample is around 0.9 g/L.<sup>5e</sup> The  $\beta$ -CD dimers **2a** and **2b** were synthesized as described in detail elsewhere.<sup>7</sup>

**Titration Calorimetry.** Isothermal titration microcalorimetry (ITC) was performed using a model 4200 microcalorimeter from Calorimetry Sciences Corp. (American Fork, UT). In individual titrations, injections of 10  $\mu$ L of the hydrophobic guest molecule were added from the computer-controlled 250

\* Corresponding author.

<sup>†</sup> UMR CNRS 8642 24.

<sup>‡</sup> UMR CNRS 7615.

<sup>§</sup> CERMAV-CNRS.

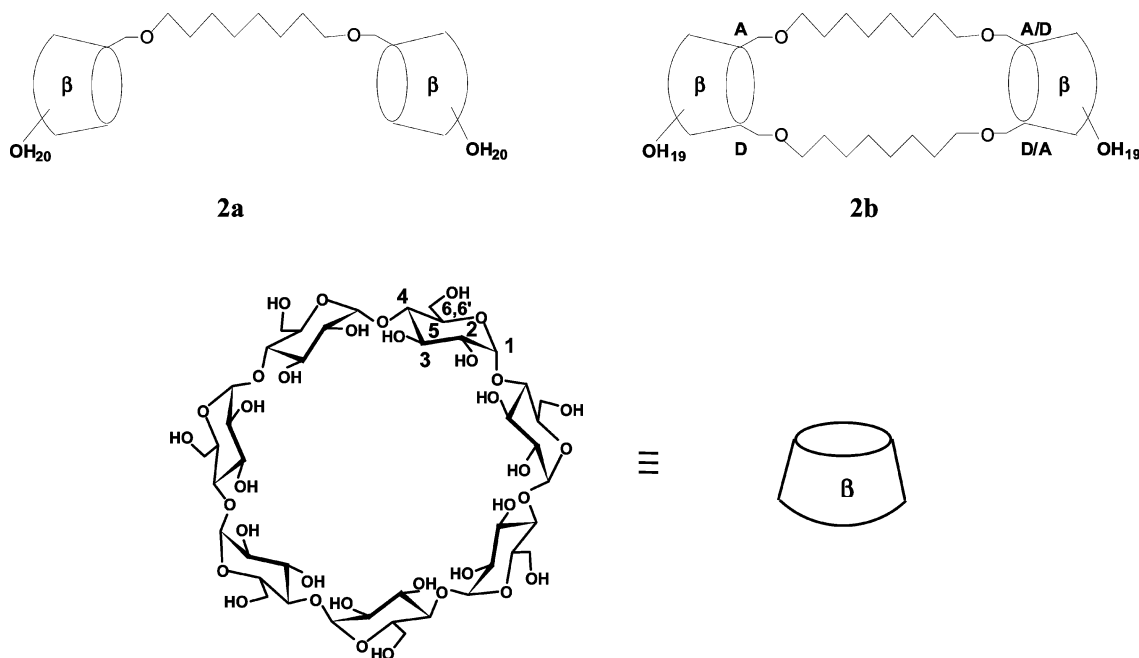


**Figure 2.** Structure of  $\beta$ -CD homodimers **2a** and **2b**. The  $\beta$ -CD cavity is represented as a truncated cone with the primary hydroxyl groups (OH-6) on the smaller rim.

$\mu$ L microsyringe at an interval of 5 min into the cyclodextrin (natural  $\beta$ -CD or  $\beta$ -CD dimer **2a**, **2b**) solution in phosphate buffer pH 7 (cell volume = 1.3 mL), while stirring at 250 rpm at 25 °C. The relative concentrations of the two solutions were adapted to the association constant and the availability of the CD cavities. The observed heat effects under identical injections of the guest molecule into a cell containing only the solvent were identical to the heat signals at the end of titration, after the saturation is reached. The raw experimental data were presented as the amount of heat produced per second following each injection of the CD molecule as a function of time. The amount of heat produced per injection was calculated by integration of the area under individual peaks by the instrument software, after taking into account heat of dilution. The experimental data were fitted to a theoretical titration curve using the instrument software, with  $\Delta H^0$  (the enthalpy change in kJ/mol),  $K_a$  (the association constant in L/mol), and  $n$  (complex stoichiometry) as adjustable parameters.

**NMR Spectroscopy.**  $^1\text{H}$  NMR experiments were performed using a Bruker DRX500 spectrometer operating at 500 MHz. 1D NMR spectra were collected using 16K data points. 2D T-ROESY and TOCSY experiments were acquired using 2K data points and 256 time increments. The phase sensitive time proportional phase incrementation method (TPPI method) was used, and processing resulted in a  $1\text{K} \times 1\text{K}$  (real–real) matrix. Chemical shifts are given relative to external tetramethylsilane (TMS = 0 ppm), and calibration was performed using the signal of the residual protons of the solvent as a secondary reference. Deuterium oxide and deuterated dimethyl sulfoxide were obtained from SDS (Vitry, France). Details concerning experimental conditions are given in the figure captions.

**Rheological Experiments.** The steady shear flow properties of solutions of adamantane–chitosan in the absence and in the presence of CD dimer **2a** or **2b** were measured using a low shear viscometer (LS30 from Contraves) or a cone–plate rheometer (AR1000 from TA Instruments), depending on the sample viscosity. The cones used have a diameter of 4 cm and an angle of 3°59' or a diameter of 6 cm and an angle of 1°, and they were equipped with a cap to avoid solvent vaporization. The solutions of adamantane-grafted chitosan and CD dimers **2a** and **2b** were prepared separately in 0.3 M  $\text{CH}_3\text{COOH}$ /0.03 M  $\text{CH}_3\text{COONa}$ , a good solvent of chitosan. The dissolution time of adamantane–chitosan was at least 1 day at room temperature. The CD dimers were dissolved in the minimum amount of solvent (65 mg/mL for **2a** and 70 mg/mL for **2b**) to avoid dilution of the polymer solution after their addition under

stirring. After each addition, the samples were allowed to rest for at least 1 h before the measurement.

**Dynamic Light Scattering.** Dynamic light scattering (DLS) measurements were performed using an ALV5000 multibit, multitau full digital correlator in combination with a MALVERN goniometer and an ALV-SIPC photomultiplier. The incident light source was an ionized argon laser (Spectra Physics 2016) emitting a vertically polarized light at a wavelength  $\lambda = 514.5$  nm. Polymer solutions investigated at 25 °C were prepared at the concentration of 2.5 g/L in 0.3 M  $\text{CH}_3\text{COOH}$ /0.03 M  $\text{CH}_3\text{COONa}$  and filtered on ANOTOP filters (porosity 0.2  $\mu\text{m}$ ) prior to measurements. The intensity autocorrelation functions ( $g_2(t, \theta)$ ) measured at a given angle ( $\theta$ ) were analyzed thanks to the REPES routine<sup>8</sup> which allows their analysis in terms of a continuous distribution of relaxation times without assuming a specific shape:

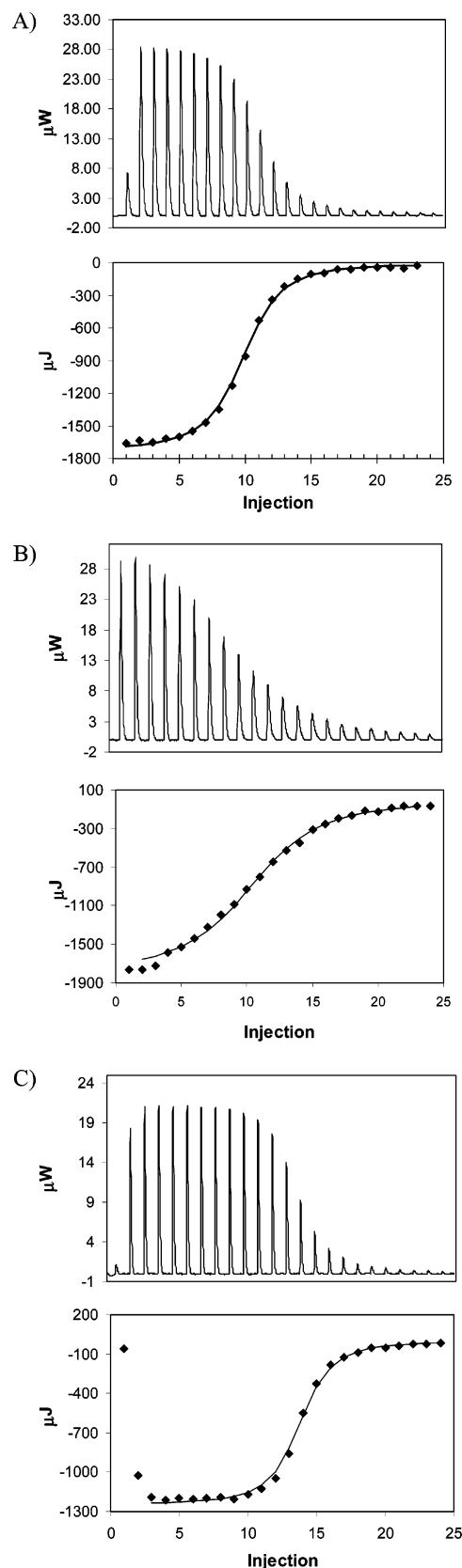
$$g_1(t, \theta) = \int_0^\infty A(\tau) \exp(-t/\tau) d\tau \quad (1)$$

Here ( $g_1(t, \theta)$ ) is the normalized electric field autocorrelation function related to ( $g_2(t, \theta)$ ) via the Siegert relation.<sup>9</sup> As detailed in the following, all the distributions of relaxation times are characterized by two peaks. The average relaxation times for the fast ( $\tau_{\text{fast}}$ ) and the slow ( $\tau_{\text{slow}}$ ) components are  $q^2$  dependent along the angular range investigated (from 30° to 140°), meaning that diffusive motions are probed.  $q$  is the wave vector defined as  $q = (4\pi n \sin(\theta/2))/\lambda$ , where  $n$  is the refractive index of the solvent. Estimates of the apparent cooperative diffusion coefficients for both relaxation processes thus may be obtained through  $D_{\text{app}}^i = \tau_i/q^2$ , where  $i$  represents the fast or the slow mode of relaxation.

## Results and Discussion

**Binding Properties of CD Dimers with Small Organic Molecules.** The synthesis of the CD homodimers **2a** and **2b** has recently been described.<sup>7</sup> In these dimers, the cyclodextrins are connected through their primary sides. Although cooperation between the two cavities may be less favored in this geometry than when CDs are connected through the broader secondary side, the advantage of such a geometry is the potential ability of the CDs to efficiently cross-link hydrophobically modified polymers since complexation of hydro-

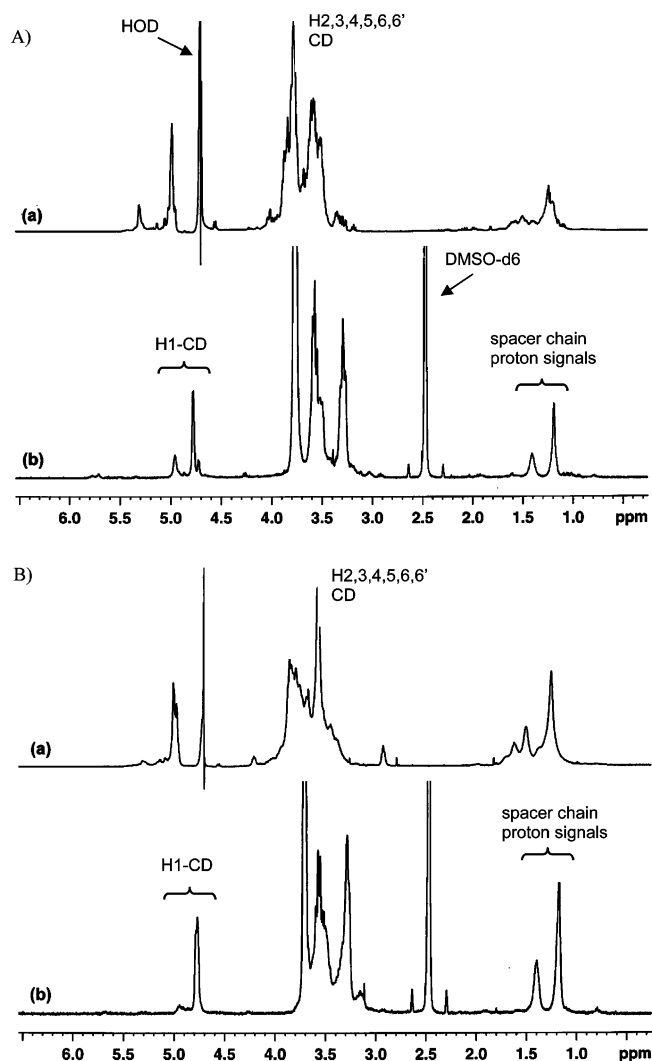
phobic guest molecules usually takes place through the wider secondary side. Moreover, unlike the majority of CD dimers that have been described to date, the dimer **2b** presents the characteristic structural feature of being doubly bridged.<sup>10</sup> Consequently, it can be assumed that the imposed mutual orientation of the two CD cavities in this dimer, compared to the conformationally much more flexible singly bridged dimer **2a**, might lead to different binding properties. We first examined the interaction of these two CD dimers with small organic guest molecules by isothermal titration calorimetry and <sup>1</sup>H NMR. Figure 3 compares the data obtained for the calorimetric titration at 25 °C of dimers **2a** and **2b** and natural  $\beta$ -CD with sodium adamantane acetate (AD), which is known to form a very strong 1:1 complex with the latter. In the case of natural  $\beta$ -CD, exothermic heat is produced after each injection of adamantane acetate. The magnitude of the released heat is nearly constant for the first injections where adamantane is almost completely bound to  $\beta$ -CD, being in large excess. Then, it decreases rapidly until the last injection, corresponding to almost complete complexation of  $\beta$ -CD. Thus, after the 24 injections of adamantane acetate, that is, addition of 2.17 mol equiv of adamantane with respect to  $\beta$ -CD, the CD cavities are saturated. In the case of dimer **2b**, although the thermogram looks similar to that obtained with natural  $\beta$ -CD, it can be noticed that saturation of the CD cavities occurs when only 0.68 mol equiv of adamantane with respect to the CD cavity is added, suggesting that one part of the CD cavities is not available for inclusion. Similar results are also obtained with dimer **2a** since complete complexation takes place after addition of only 1.1 mol equiv of adamantane with respect to the CD cavity. Moreover, for dimer **2a**, the magnitude of the released heat decreases more rapidly with the first injections reflecting a lower complexation efficiency. Indeed, the fact that the released heat is not maximum during the first injections, when CD cavities are in large excess with respect to added adamantane, suggests that adamantane is not completely complexed. These preliminary conclusions derived from experimental observations were fully confirmed by the thermodynamic parameters calculated from the experimental data (see Table 1). Table 1 shows that the three cyclodextrin molecules have similar  $\Delta H^0$  values, indicating similar mechanisms of binding. However, the complexation of adamantane acetate by CD dimer **2b** appears to be 3 times stronger than that by the natural  $\beta$ -CD as a result of a favorable change in entropy. This might be related to a strengthening of hydrophobic binding as already reported for other CD derivatives with hydrophobic substituents.<sup>11,12</sup> Indeed, it can be assumed that the presence of the two C8 hydrophobic chains connecting the CD cavities on their primary side may strengthen hydrophobic interactions with hydrophobic adamantane. This idea was further supported by the fact that in the case of complexation with aromatic (+)-catechin, involving dipole–dipole interactions in addition to hydrophobic interactions, the association constants are similar for natural  $\beta$ -CD and dimer **2b** (data not shown). On the other hand, it can be observed that the bridging of the two CDs by only one octamethylene chain does not favor the complexation ability of the cavities. Concerning the stoichiometry of the complexes, large discrepancies appear between the theoretical and experimental values. The  $n$  values of 1.02 and 0.80 instead of 2, found



**Figure 3.** Calorimetric titration of the binding of sodium adamantane acetate to (A) natural  $\beta$ -CD, (B)  $\beta$ -CD dimer **2a**, and (C)  $\beta$ -CD dimer **2b**. Upper halves: raw data obtained for 24 automatic injections, each of 10  $\mu$ L, of adamantane acetate to the CD molecule (the concentration of the host and guest molecules in phosphate buffer (pH 7) for each case is indicated in Table 1). Lower halves: the integrated curve showing experimental points and the best fit for titration of the natural CD and CD dimers.

**Table 1. Thermodynamic Parameters for Inclusion Complex Formation of Sodium Adamantane Acetate with Natural  $\beta$ -CD and  $\beta$ -CD Dimers **2a** and **2b****

CD derivative	CD cavity concn (mM)	AD concn (mM)	$K_a \times 10^{-4}$ (M <sup>-1</sup> )	$\Delta H^0$ (kJ/mol)	$T\Delta S^0$ (kJ/mol)	$n$ (nAD:1CD derivative)
natural $\beta$ -CD	0.56	6.59	7.96 ( $\pm 0.05$ )	-26.2 ( $\pm 0.4$ )	1.76	0.90 ( $\pm 0.01$ )
dimer <b>2a</b>	1.2	7.2	2.32 ( $\pm 0.07$ )	-25.0 ( $\pm 0.4$ )	-0.09	1.02 ( $\pm 0.01$ )
dimer <b>2b</b>	1.2	4.4	26.42 ( $\pm 0.05$ )	-28.2 ( $\pm 0.4$ )	2.73	0.80 ( $\pm 0.01$ )

**Figure 4.**  $^1\text{H}$  NMR spectra (400 MHz, 25  $^\circ\text{C}$ ) of (A)  $\beta$ -CD dimer **2a** (3 mg/mL) and (B)  $\beta$ -CD dimer **2b** (3 mg/mL) (a) in  $\text{D}_2\text{O}$  and (b) in  $\text{DMSO}-d_6$  containing two drops of  $\text{D}_2\text{O}$ .

for dimers **2a** and **2b**, respectively, indicate that one part of the CD cavities (50% for **2a** and 60% for **2b**) is unavailable or inactive for binding.

To get more information about the complexation behavior of dimers **2a** and **2b**,  $^1\text{H}$  NMR spectra of these compounds alone and in the presence of guest molecules were recorded. From Figure 4, it can be seen that the NMR spectra of dimers **2a** and **2b** in  $\text{D}_2\text{O}$  strongly differ from those in  $\text{DMSO}-d_6$ . For both compounds, the octamethylene chains display considerable dispersion in  $\text{D}_2\text{O}$ . Conversely, in  $\text{DMSO}$ , this spectral dispersion collapses. Since  $\text{DMSO}$  has a strong solvating power for the CD cavity, it is known to preclude the formation of inclusion complexes. This behavior thus suggests inclusion of the octamethylene spacer in the CD cavity for both CD dimers. Similar observations have been already reported for  $\beta$ -CD dimers connected through either the secondary or the primary side by an aliphatic moiety.<sup>3c,3d,13</sup> More direct evidence for the formation of

inclusion complexes can be derived from the direct observation of spatial proximities between protons of the linkers and the H-3 and H-5 protons located in the CD cavity. This can be achieved by 2D T-ROESY experiments<sup>14</sup> dedicated to evidence dipolar interactions (nuclear Overhauser effects). Partial T-ROESY contour plots together with partial 2D TOCSY contour plots of **2a** and **2b** in  $\text{D}_2\text{O}$  are displayed in Figure 5. 2D TOCSY experiments, based upon stepwise magnetization transfers from anomeric protons,<sup>15</sup> allowed the observation of the H-3 and H-5 cavity protons of cyclodextrin which cannot be distinguished in the complicated 1D  $^1\text{H}$  NMR spectrum. The presence of strong cross-peaks between the protons of the C8 chain and the H-3 and maybe H-5 protons of cyclodextrin fully supports the inclusion of spacers in CD cavities. This could partly explain the observed unavailability of about 50% of the cavities in both dimers. Since interaction between the CD cavity and the octamethylene chain implies the latter to bend, insertion likely occurs through the wider side. This is moreover supported by the clear observation of dipolar contacts between the protons of the chain and the H-3 CD protons located near the wider secondary side. Consequently, the CD cavities in a dimer would be occupied by the linker of other dimers. This complexation between several dimer molecules may lead to the formation of large aggregates, making some CD cavities inaccessible for inclusion of external guest molecules. Furthermore, aggregates may also result from the amphiphilic nature of the CD dimers and may be stabilized by hydrogen bonds between the CD cavities. Thus, this could partly explain why, from the calorimetry experiments, one part of the CD cavities is unavailable for inclusion of adamantane acetate, despite its very high affinity for the  $\beta$ -CD cavity.

**Interaction of CD Dimers with Adamantane-Grafted Chitosan as a Guest Macromolecule.** In the previous section, we have examined complexation of dimers **2a** and **2b** with small organic molecules. It was demonstrated for both CD derivatives that about half of the CD cavities are inactive for complexation. This was attributed to the formation of aggregates of dimers promoted by their amphiphilic nature, the inclusion of the octamethylene spacer, and hydrogen bond interactions between the cavities. Nevertheless, the benefit of doubly bridging the CDs cavities was evidenced by the large increase in binding strength (higher value of  $K$ , Table 1) of the CD cavities in dimer **2b** toward hydrophobic adamantane. In contrast, an opposite effect was observed by singly bridging the CD cavities according to dimer **2a**. We further compared the complexation behavior of both dimers **2a** and **2b** toward adamantane-grafted chitosan as a guest macromolecule. For this purpose, effects of adding dimers **2a** and **2b** on the solution viscosity of AD-chitosan were studied. Viscosity measurements were performed keeping the polymer concentration  $C$  constant ( $1 \text{ g/L} \leq C \leq 5 \text{ g/L}$ ), while progressively increasing the concentration of **2a** or **2b**. Figures 6 and 7 display the apparent viscosity vs shear rate for solutions of AD-chitosan ( $C = 2.5 \text{ g/L}$ ) alone



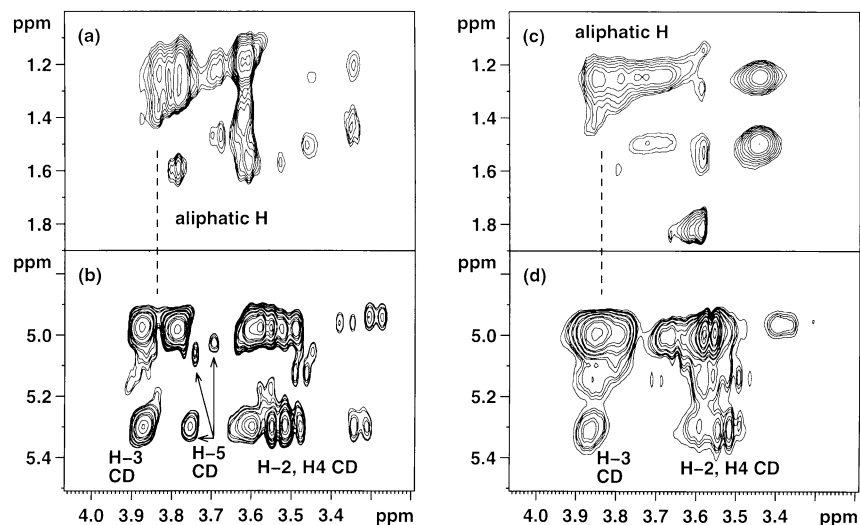


**Figure 5.** Partial contour plots of 2D T-ROESY experiments (500 MHz, 25 °C, D<sub>2</sub>O, 150 ms spin-lock time at 16 dB attenuation) performed on (a)  $\beta$ -CD dimer **2a** (2 mM) and (c)  $\beta$ -CD dimer **2b** (2 mM). Partial contour plots of 2D TOCSY experiments (500 MHz, 25 °C, D<sub>2</sub>O, 80 ms mixing time) performed on (b)  $\beta$ -CD dimer **2a** (2 mM) and (d)  $\beta$ -CD dimer **2b** (2 mM).

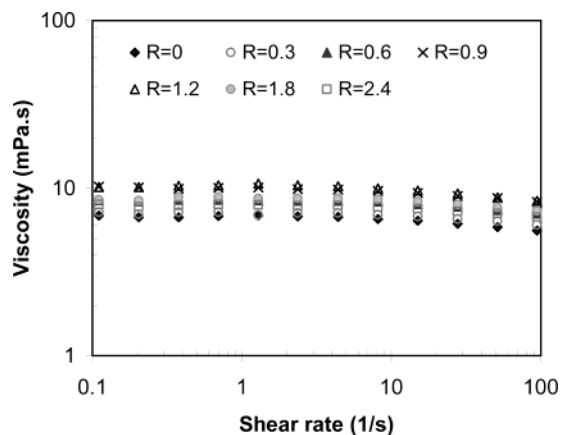


**Figure 6.** Viscosity dependence on shear rate for solutions of AD-chitosan ( $C = 2.5$  g/L, 0.3 M CH<sub>3</sub>COOH/0.03 M CH<sub>3</sub>COONa, 25 °C) in the absence and in the presence of increasing  $\beta$ -CD dimer **2a**.  $R$  refers to the [CD]/[AD] ratio.

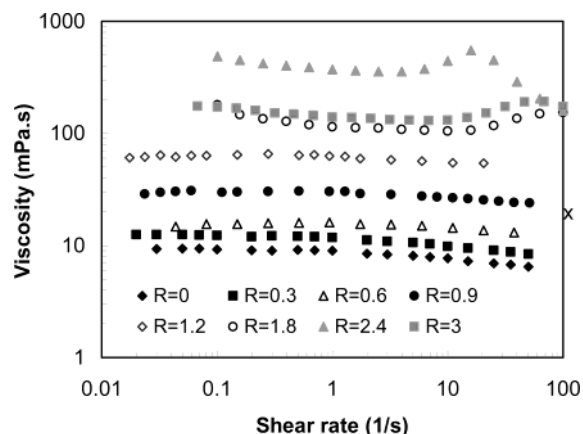


**Figure 7.** Viscosity dependence on shear rate for solutions of AD-chitosan ( $C = 2.5$  g/L, 0.3 M CH<sub>3</sub>COOH/0.03 M CH<sub>3</sub>COONa, 25 °C) in the absence and in the presence of increasing  $\beta$ -CD dimer **2b**.

and in the presence of increasing content of CD dimer **2a** and **2b**. A viscosity enhancement in the case of both CD dimers can be easily seen, which can be reasonably attributed to cross-linking of AD-chitosan chains through complexation of CD dimers with grafted ADs. Neverthe-

less, the highest viscosity values are significantly different for the two dimers. Another important observation is the appearance of a shear thickening behavior (i.e., a viscosity increase with shear rate) at intermediate shear rates for dimer **2b**/AD-chitosan mixtures above a [CD]/[AD] ratio  $R$  of 1.2. Moreover, as the [CD]/[AD] ratio increases from 1.8 to 2.4, which seems to be the optimal value for viscosity enhancement, the onset of shear thickening is displaced toward lower shear rate values, while the magnitude of the shear thickening effect remains approximately the same. The shear-thickening zone is shown to be followed by shear thinning. As the [CD]/[AD] ratio further increases, the onset of shear thickening shifts again to higher shear rates, the magnitude of shear thickening effect being nearly the same. In fact, the shear-thickening behavior closely follows that of the zero-shear viscosity  $\eta_0$  with the lowest onset of shear thickening at the [CD]/[AD] ratio for which  $\eta_0$  is maximum. Shear-thickening effects have already been encountered for macromolecules near  $\theta$  conditions<sup>16</sup> and associating polymers.<sup>17</sup> Different mechanisms including shear-induced cross-linking,<sup>18</sup> shear-induced increase in the density of mechanically active chains,<sup>19</sup> and/or shear-induced chain stretching<sup>20</sup> have been proposed to explain the shear thickening. In the present case, we can postulate that elongation of AD-chitosan chains render some adamantane groups available for the formation of additional interchain cross-links through complexation with CD dimer **2b**. Thus, for the viscosity maximum, the appearance at a lower shear rate of the shear thickening can be related to an increased probability of the interchain cross-links due to the increase of both CD and AD local concentrations. It is surprising that such a behavior is not observed in the case of dimer **2a**, which is also able to cross-link AD-chitosan chains. This difference may be related to the higher rigidity of doubly linked dimer **2b** with respect to singly bridged dimer **2a**, favoring interchain complex formation under shear flow. Concerning the enhancement of viscosity, as already mentioned, a much higher efficiency is observed for dimer **2b**. This is more clearly illustrated by Figure 8 showing the dependence of the zero-shear rate viscosity of AD-chitosan solutions at different concentrations on the [CD]/[AD] ratio. The greater ability of dimer **2b** to

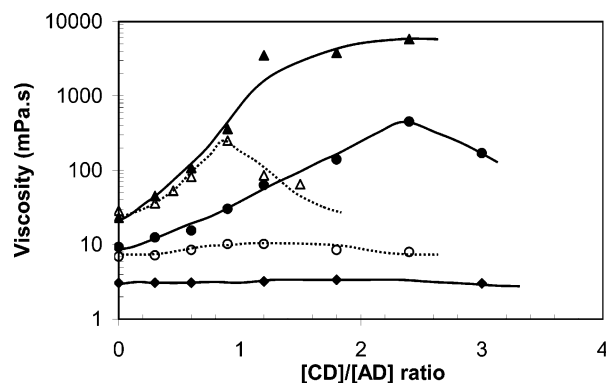


**Figure 8.** Variation of the viscosity of solutions of AD-chitosan in the range of concentrations from 1 to 5 g/L (0.3 M  $\text{CH}_3\text{COOH}/0.03 \text{ M } \text{CH}_3\text{COONa}$ , 25 °C) with the  $[\text{CD}]/[\text{AD}]$  ratio (i.e., with increasing concentration of CD dimers **2a** and **2b**):  $\blacklozenge$ , dimer **2b**/AD-chit 1 g/L;  $\bullet$ , dimer **2b**/AD-chit 2.5 g/L;  $\blacktriangle$ , dimer **2b**/AD-chit 5 g/L;  $\triangle$ , dimer **2a**/AD-chit 5 g/L;  $\circ$ , dimer **2a**/AD-chit 2.5 g/L.

enhance the solution viscosity of AD-chitosan might be explained by a higher cross-link density in the case of this CD derivative due to the greater binding strength of its CD cavities toward adamantane than those of dimer **2a**, as discussed in the previous section. This may be also related to the lower molecular flexibility of **2b** as additional cross-links are easily obtained when some AD moieties are rendered available for complexation. Another parameter, which might be also taken into account to explain the better efficiency observed for dimer **2b**, is the lifetime of the cross-links. From Figure 8, it can be also observed that the magnitude of the viscosity enhancement is an increasing function of polymer concentration. As observed in the study of the cross-linking of cyclodextrin-grafted chitosan by flexible poly(ethylene glycol)-diadamantane, viscosity increases are only clearly observed for AD-chitosan concentrations higher than 1 g/L, which means that interchain bridging can only be effective in the range of concentrations larger than the polymer overlap concentration  $C^*$  ( $\sim 0.9 \text{ g/L}$ ). The correlation between the position of the maximum of viscosity and the  $[\text{CD}]/[\text{AD}]$  ratio for both dimers is difficult to assess. Nevertheless, the decrease of viscosity above the optimal  $[\text{CD}]/[\text{AD}]$  ratio for viscosity enhancement can be seen as the result of an increase of CD dimer monocomplexation to the detriment of dicomplexation.

These conclusions based on the measurement of a macroscopic parameter such as the viscosity of the solutions also hold when results from dynamic light scattering which probes the solutions at a mesoscopic scale are considered. Figure 9 shows the distributions of the relaxation times obtained for AD-chitosan solutions at 2.5 g/L with different  $[\text{CD}]/[\text{AD}]$  ratios of both dimers **2a** and **2b** ( $\theta = 90^\circ$ ). Whatever the ratio  $[\text{CD}]/[\text{AD}]$  is, the distributions of the relaxation times are clearly bimodal. This latter fact has already been reported by Buhler et al.<sup>21</sup> for solutions of the unmodified homologue chitosan above the critical overlap concentration ( $C^* = 0.9 \text{ g/L}$ ) in 0.3 M  $\text{CH}_3\text{COOH}/0.05 \text{ M } \text{CH}_3\text{COONa}$ . According to these authors, the fast mode of relaxation has been attributed to the cooperative motion of entangled polymer chains which can be assimilated to the breathing of the semidilute network under the effect of the osmotic pressure ( $D_{\text{fast}} = 3.8 \times 10^{-11} \text{ m}^2/\text{s}$  at 2.5 g/L), whereas the slow mode of relaxation is claimed to be due to the formation of

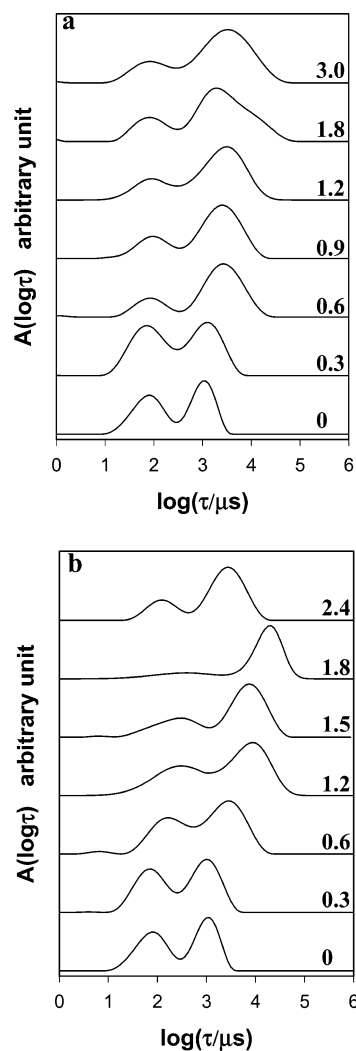


**Figure 9.** Distribution of the relaxation times obtained from DLS at  $90^\circ$  for different values of the  $[\text{CD}]/[\text{AD}]$  ratio for (a) CD dimer **2a** and (b) CD dimer **2b**; the concentration of AD-chitosan is 2.5 g/L.

physical polymer associations related to the high rigidity of the backbone ( $D_{\text{slow}} = 1.5 \times 10^{-12} \text{ m}^2/\text{s}$  at 2.5 g/L). For the solutions of the AD-chitosan studied at a lower salt concentration (0.03 M  $\text{CH}_3\text{COONa}$ ), values for both modes of relaxation  $D_{\text{fast}} = 3.1 \times 10^{-11} \text{ m}^2/\text{s}$  and  $D_{\text{slow}} = 2.0 \times 10^{-12} \text{ m}^2/\text{s}$  fairly agree with the work of Buhler et al., meaning that the hydrophobic modification has only a weak effect on the overall conformation of the polymer chains in solution as already pointed out in previous works.<sup>5e,22</sup>

The influence of the addition of dimers **2a** and **2b** on the dynamics of AD-chitosan solutions clearly depends on their chemical nature as pointed out in Figure 9. Addition of **2a** to the AD-chitosan solution weakly affects the average relaxation time for the fast mode whereas the slow mode is clearly slowed down by the increase of the  $[\text{CD}]/[\text{AD}]$  ratio (Figure 9a). When compound **2b** is considered (Figure 9b), both modes of relaxation are slowed down as long as the  $[\text{CD}]/[\text{AD}]$  ratio  $R$  remains lower than 1.8. Then, above this value, both average times of relaxation decrease.

A clearer image of the influence of the addition of CD dimers **2a** and **2b** on the dynamics of the solutions may be gained when considering the variation of the apparent diffusion coefficients with the  $[\text{CD}]/[\text{AD}]$  ratio (see Figures 10 and 11). For the fast mode of relaxation, the

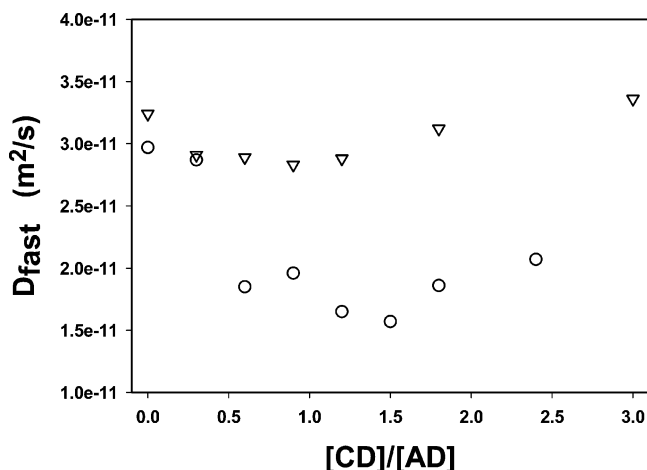


**Figure 10.** Variation of the apparent diffusion coefficient for the fast mode of relaxation obtained from DLS with the  $[CD]/[AD]$  ratio when CD dimer **2a** (triangles) or CD dimer **2b** (circles) is added.

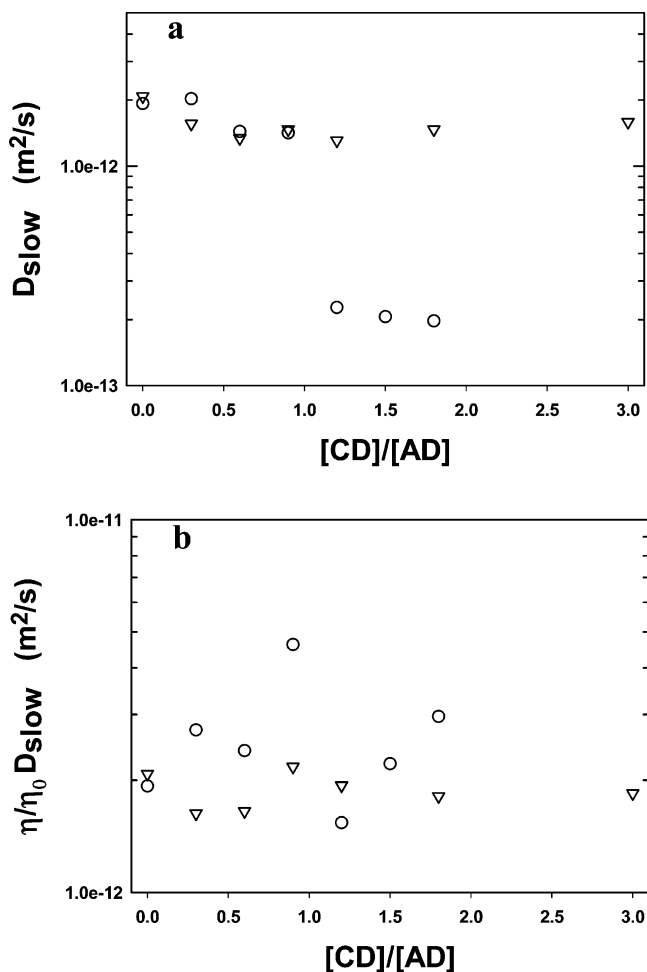


**Figure 11.** Variation of the apparent diffusion coefficient for the slow mode of relaxation obtained from DLS with the  $[CD]/[AD]$  ratio when CD dimer **2a** (triangles) or CD dimer **2b** (circles) is added. Data have been rescaled by the macroscopic viscosity of the solutions in (b) (see text).

apparent diffusion coefficient slightly decreases by 13% when dimer **2a** is added and remains roughly constant for  $R$  values ranging from 0.3 to 1.2. Then, above 1.2,  $D_{app}^{fast}$  increases. For dimer **2b**, the decrease of  $D_{app}^{fast}$  with  $R$  is much more pronounced (almost 50%) and is a more cooperative phenomenon. Furthermore,  $D_{app}^{fast}$  increases

for  $R$  values higher than 1.5. These tendencies must be closely related to the variation of the viscosity observed in the presence of both dimers. The greater binding strength showed by the CD cavities of compound **2b** toward adamantane and the higher rigidity of dimer **2b** makes it more efficient as a complexing agent. Thus, at the mesoscopic scale dimer **2b** slows down the dynamics of AD–chitosan in a larger extent than dimer **2a**, which results in a higher viscosity enhancement. Furthermore, above an optimal  $[CD]/[AD]$  ratio corresponding likely to the complete complexation of the accessible grafted adamantane groups, the predominance of monocomplexation of dimers with respect to their dicomplexation results in both cases in an increase of  $D_{app}^{fast}$ .

Regarding now the slow mode of relaxation obtained from DLS, Figure 11a displays the variation of its apparent diffusion coefficient with the ratio  $[CD]/[AD]$ . It can be seen that the slow mode is deeply affected by the addition of both CD dimers and that this effect is tremendous in the case of dimer **2b**. Nevertheless, it should be emphasized that considering the size of the scattering species responsible for the slow mode, the viscosity which is felt locally by these species is rather the macroscopic viscosity of the solutions than the viscosity of the solvent. Accordingly, the data have been rescaled by the macroscopic viscosity  $\eta$  of the samples as shown by Figure 11b ( $\eta_0$  is the viscosity for the solution of AD–chitosan at 2.5 g/L). For both dimers, one can clearly see that the diffusion coefficient is roughly constant over the whole  $R$  range investigated, which means that dimers **2a** and **2b** have nearly no influence on the size of the aggregates that may be formed in the initial polymeric solution by some physical associations. Actually, this situation is reminiscent of the case encountered with hydrophobically end-capped poly(ethylene oxide) dissolved in water where spurious PEO aggregates turn out to be slowed down by the huge increase in the viscosity of the solution with the concentration due to the associating properties of the polymer.<sup>23</sup>

In conclusion, we have demonstrated by a combination of viscometric and DLS studies that CD homodimers can efficiently increase the viscosity of a hydrophobically modified polymer, AD–chitosan, through the formation of physical cross-links. The ability of the CD dimers to cross-link AD–chitosan chains was shown to be closely related to their molecular architecture. In fact, the number of aliphatic spacers (1 or 2) connecting the two CD cavities changes their inclusion properties as shown by isothermal titration calorimetry, and this has a pronounced effect on the stability of the complex and hence on the ability of dimers to enhance the viscosity of AD–chitosan solutions. The cross-linking properties of more complex CD derivatives are currently under investigation and will be reported in the near future.

## References and Notes

- (1) Wenz, G. *Angew. Chem., Int. Ed. Engl.* **1994**, *33*, 803.
- (2) Szejtli, J. *Chem. Rev.* **1998**, *98*, 1743.
- (3) (a) Breslow, R.; Zhang, B. *J. Am. Chem. Soc.* **1993**, *114*, 5882. (b) Breslow, R.; Zhang, B. *J. Am. Chem. Soc.* **1994**, *116*, 7893. (c) Venema, F.; Baselier, C. M.; Feiters, M. C.; Nolte, R. J. M. *Tetrahedron Lett.* **1994**, *35*, 8661. (d) Venema, F.; Nelissen, H. F. M.; Berthault, P.; Birlirakis, N.; Rowan, A. E.; Feiters, M. C.; Nolte, R. J. M. *Chem.—Eur. J.* **1998**, *4*, 2237.
- (4) (a) Ueno, A. *Supramol. Sci.* **1996**, *3*, 31. (b) Corradini, R.; Dossena, A.; Galaverna, G.; Marchelli, R.; Panagia, A.; Sartor, G. *J. Org. Chem.* **1997**, *62*, 6283. (c) Nelissen, H. F. M.

- Venema, F.; Uittenbogaard, R. M.; Feiters, M. C.; Nolte, R. J. M. *J. Chem. Soc., Perkin Trans. 2* **1997**, 2045. (d) de Jong, M. R.; Engbersen, J. F. J.; Huskens, J.; Reinhoudt, D. N. *Chem.-Eur. J.* **2000**, *6*, 4034.
- (5) (a) Huh, K. M.; Ooya, T.; Lee, W. K.; Sasaki, S.; Kwon, I. C.; Jeong, S. Y.; Yui, N. *Macromolecules* **2001**, *34*, 8657. (b) Amiel, C.; Sebille, B. *J. Inclusion Phenom. Mol. Recognit. Chem.* **1996**, *25*, 61. (c) Sandier, A.; Brown, W.; Mays, H.; Amiel, C. *Langmuir* **2000**, *16*, 1634. (d) Weickenmeier, M.; Wenz, G.; Huff, J. *Macromol. Rapid Commun.* **1997**, *18*, 1117. (e) Auzély-Velty, R.; Rinaudo, M. *Macromolecules* **2002**, *35*, 7955. (f) Choi, H. S.; Huh, K. M.; Ooya, T.; Yui, N. *J. Am. Chem. Soc.* **2003**, *125*, 6350. (g) Choi, H. S.; Ooya, T.; Sasaki, S.; Yui, N. *Macromolecules* **2003**, *36*, 5342.
- (6) For example, see: (a) Yuan, D.-Q.; Lu, J.; Atsumi, M.; Izuka, A.; Kai, M.; Fujita, K. *Chem. Commun.* **2002**, 730. (b) Yan, J.-M.; Atsumi, M.; Yuan, D.-Q.; Fujita, K. *Helv. Chim. Acta* **2002**, *85*, 1496. (c) Mulder, A.; Jukovic, A.; Lucas, L. N.; van Esch, J.; Feringa, B. L.; Huskens, J.; Reinhoudt, D. N. *Chem. Commun.* **2002**, 2734. (d) Nelissen, H. F. M.; Feiters, M. C.; Nolte, R. J. M. *J. Org. Chem.* **2002**, *67*, 5901. (e) References (4) in (7).
- (7) Lecourt, T.; Mallet, J. M.; Sinay, P. *Eur. J. Org. Chem.* **2003**, 4553.
- (8) Stepanek, P. *Dynamic Light Scattering*; Brown, W., Ed.; Oxford University Press: New York, 1993; Chapter 4.
- (9) Berne, B.; Pecora, R. *Dynamic Light Scattering*; Wiley: New York, 1976.
- (10) (a) Tabushi, I.; Kuroda, Y.; Shimokawa, K. *J. Am. Chem. Soc.* **1979**, *101*, 1614. (b) Brelow, R.; Chung, S. J. *J. Am. Chem. Soc.* **1990**, *112*, 9659. (c) Breslow, R.; Halfon, S.; Zhang, B. *Tetrahedron* **1995**, *51*, 377. (d) Sasaki, K.; Nagasaka, M.; Kuroda, Y. *Chem. Commun.* **2001**, 2630. (e) Lecourt, T.; Mallet, J.-M.; Sinay, P. *Tetrahedron Lett.* **2002**, *43*, 5533. (f) Yuan, D.-Q.; Immel, S.; Koga, K.; Yamagushi, M.; Fujita, K. *Chem.-Eur. J.* **2003**, *9*, 3501.
- (11) Emert, J.; Breslow, R. *J. Am. Chem. Soc.* **1975**, *97*, 670.
- (12) Tabushi, I.; Shimokawa, K.; Shimizu, N.; Shirakata, H.; Fujita, K. *J. Am. Chem. Soc.* **1976**, *98*, 7855.
- (13) Yamamura, H.; Yamada, S.; Kohno, K.; Okuda, N.; Araki, S.; Kobayashi, K.; Katakai, R.; Kano, K.; Kawai, M. *J. Chem. Soc., Perkin Trans. 1* **1999**, 2943.
- (14) Hwang, T. L.; Shaka, A. J. *J. Magn. Reson., Ser. B* **1993**, *102*, 155.
- (15) Bax, A.; Davis, D. G. *J. Magn. Reson.* **1985**, *65*, 355.
- (16) (a) Layec-Raphalen, M. N.; Wolff, C. *J. Non-Newtonian Fluid Mech.* **1976**, *1*, 159. (b) Yanase, H.; Moldenaers, P.; Mewis, J.; VanEgmond, J.; Fuller, G. *Rheol. Acta* **1991**, *30*, 89. (c) Moldenaers, P.; Yanase, H.; Mewis, J.; Fuller, G.; Lee, C. S.; Magda, J. *Rheol. Acta* **1993**, *32*, 1. (d) Vrahopoulou, E. P.; McHugh, A. J. *J. Non-Newtonian Fluid Mech.* **1987**, *25*, 157. (e) Dupuis, C.; Wolff, C. *J. Rheol.* **1993**, *37*, 587. (f) Dupuis, D.; Lewandowski, F. Y.; Steiert, P.; Wolff, C. *J. Non-Newtonian Fluid Mech.* **1994**, *54*, 11. (g) Eliassaf, J.; Silberberg, A.; Katchalsky, A. *Nature (London)* **1955**, *176*, 1119.
- (17) (a) Volpert, E.; Selb, J.; Candau, F. *Macromolecules* **1996**, *29*, 1452. (b) Siquin, A.; Hubert, P.; Marchal, P.; Choplin, L.; Dellacherie, E. *Colloids Surf. A: Physicochem. Eng. Aspects* **1996**, *112*, 193. (c) English, R. J.; Gulati, H. S.; Jenkins, R. D.; Khan, S. A. *J. Rheol.* **1997**, *41*, 427. (d) Tam, K. C.; Jenkins, R. D.; Winnik, M. A.; Basset, D. R. *Macromolecules* **1998**, *31*, 4149. (e) Vittadello, S. T.; Biggs, S. *Macromolecules* **1998**, *31*, 7691. (f) Tam, K. C.; Guo, L.; Jenkins, R. D.; Basset, D. R. *Polymer* **1999**, *40*, 6369. (g) Maerker, J. M.; Sinton, S. W. *J. Rheol.* **1986**, *30*, 77. (h) Van Egmond, J. W. *Curr. Opin. Colloid Interface Sci.* **1998**, *3*, 385. (i) Kujawa, P.; Rosiak, J. M.; Selb, J.; Candau, F. *Macromol. Chem. Phys.* **2001**, *202*, 1384.
- (18) Witten, T. A.; Cohen, M. H. *Macromolecules* **1985**, *18*, 1915.
- (19) Noda, T.; Hashidzume, A.; Morishima, Y. *Langmuir* **2000**, *16*, 5324.
- (20) Marrucci, G.; Bhargava, S.; Cooper, S. L. *Macromolecules* **1993**, *26*, 6483.
- (21) Buhler, E.; Rinaudo, M. *Macromolecules* **2000**, *33*, 2098.
- (22) Charlot, A.; Auzély-Velty, R.; Rinaudo, M. *J. Phys. Chem. B* **2003**, *107*, 8248.
- (23) Chassenieux, C.; Nicolai, T.; Durand, D. *Macromolecules* **1997**, *30*, 4952.

MA049822X